

Sources and Transformation Mechanisms of Atmospheric Particulate Bound Mercury Revealed by Mercury Stable Isotopes

Chen Liu, Xuewu Fu,* Yue Xu, Hui Zhang, Xian Wu, Jonas Sommar, Leiming Zhang, Xun Wang, and Xinbin Feng



Cite This: *Environ. Sci. Technol.* 2022, 56, 5224–5233



Read Online

ACCESS |



Metrics & More



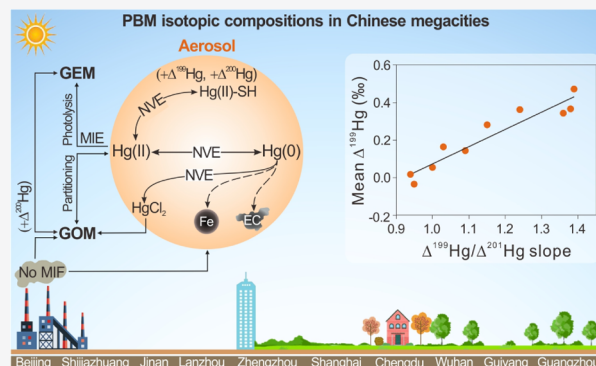
Article Recommendations



Supporting Information

ABSTRACT: This study examined the isotopic composition of particulate bound mercury (PBM) in 10 Chinese megacities and explored the associated sources and transformation mechanisms. PBM in these cities was characterized by negative $\delta^{202}\text{Hg}$ (mean: -2.00 to -0.78‰), slightly negative to highly positive $\Delta^{199}\text{Hg}$ (mean: -0.04 to 0.47‰), and slightly positive $\Delta^{200}\text{Hg}$ (mean: 0.02 to 0.06‰) values. The positive PBM $\Delta^{199}\text{Hg}$ signatures were likely caused by physiochemical reactions in aerosols. The $\Delta^{199}\text{Hg}/\Delta^{201}\text{Hg}$ ratio varied from 0.94 to 1.39 in the cities and increased with the increase in the corresponding mean $\Delta^{199}\text{Hg}_{\text{PBM}}$ value. We speculate that, in addition to the photoreduction of oxidized Hg, other transformation mechanisms in aerosols (e.g., isotope exchange, complexation, and oxidation, which express nuclear volume effects) also shape the $\Delta^{199}\text{Hg}_{\text{PBM}}$ signatures in the present study. These processes are likely enhanced in the presence of strong gas-particle partitioning of gaseous oxidized Hg (GOM) and elevated levels of redox active metals (e.g., Fe), halides, and elemental carbon. Based on $\Delta^{200}\text{Hg}_{\text{PBM}}$ data presented in this and previous studies, we estimate that large proportions ($\sim 47 \pm 22\%$) of PBM were sourced from the oxidation of gaseous elemental Hg followed by the partitioning of GOM onto aerosols globally, indicating the transformation of $\text{Hg}(0)$ to PBM as an important sink of atmospheric $\text{Hg}(0)$.

KEYWORDS: PBM, urban atmosphere, stable Hg isotope, MIF, MIE, NVE, heterogeneous Hg reactions, sources



1. INTRODUCTION

Mercury (Hg) in the atmosphere mainly exists in the forms of gaseous elemental mercury [GEM or $\text{Hg}(0)$], gaseous oxidized mercury (GOM), and particulate bound mercury (PBM). Hg directly emitted into the atmosphere from anthropogenic and natural sources or reemitted from previously deposited Hg is mostly in the form of $\text{Hg}(0)$.¹ $\text{Hg}(0)$ is much less susceptible to dry and wet removal processes as compared with GOM and PBM and is readily transported over a hemispherical scale. Oxidation of $\text{Hg}(0)$ to $\text{Hg}(\text{II})$ (GOM and PBM) in the atmosphere followed by $\text{Hg}(\text{II})$ wet and dry deposition is perceived as one of the major sinks of atmospheric $\text{Hg}(0)$.^{2,3} Hence, a complete understanding of the sources and transformation mechanisms of speciated atmospheric Hg is critical for assessing Hg cycling in the atmosphere.

Recent studies have improved our understanding of the atmospheric gas-phase Hg redox schemes,^{4–7} while the knowledge of reactions in aqueous and heterogeneous phases remains largely limited.^{7,8} In current global atmospheric Hg models, $\text{Hg}(0)$ oxidation is assumed to be mainly induced by Br and OH, and then the gaseous oxidized Hg could be either reduced back to $\text{Hg}(0)$, could persist as GOM in the atmosphere in relatively photochemically and thermally stable

$\text{Hg}(\text{I}, \text{II})$ forms, or could be captured by aerosols and cloud droplets.^{2,3,8,9} Once incorporated into aerosols and cloud droplets, $\text{Hg}(\text{I}, \text{II})$ can undergo many physiochemical transformation processes.⁷ Among viable processes, aqueous-phase $\text{Hg}(\text{II})$ photoreduction is frequently considered in modeling studies and is supposed to play important roles in the atmospheric chemistry of Hg.^{2,3,8} On the other hand, other in-aerosol processes such as re-oxidation, complexation, and adsorption, which allow $\text{Hg}(\text{II})$ to be retained as PBM, are frequently neglected in global modeling because of deficient knowledge.^{3,7,8}

Hg stable isotopes can help constrain its sources and transformation mechanisms in the natural environment because physicochemical processes induce mass dependent fractionation (MDF; $\delta^{202}\text{Hg}$ signature) and odd- and even-mass independent fractionation (MIF; $\Delta^{199}\text{Hg}$, $\Delta^{200}\text{Hg}$, and

Received: November 26, 2021

Revised: March 22, 2022

Accepted: March 28, 2022

Published: April 6, 2022



$\Delta^{201}\text{Hg}$ signatures). MDF of Hg isotopes can be caused by many physicochemical processes, including reduction, methylation/demethylation, sorption, and evaporation.¹⁰ Large odd-MIF of Hg isotopes are mainly associated with photochemical redox reactions due to the magnetic isotope effect (MIE).^{11–15} Small magnitudes of odd-MIF (e.g., <0.6‰) have also been observed in abiotic dark Hg(II) reduction, Hg(II) complexation with thiol, and abiotic dark Hg(0) oxidation (mainly due to equilibrium isotope exchange) experiments, which are accompanied by a discernible $\Delta^{199}\text{Hg}/\Delta^{201}\text{Hg}$ regression slope of ~ 1.6 compared to the MIE (slope of ~ 1.0) due to the nuclear volume effect (NVE).^{16–18} Even-MIF anomalies are mainly observed in atmospheric samples and are assumed to be exclusively produced during atmospheric redox reactions at high altitudes.^{19–22} Recently, measurements of the Hg isotopic composition in atmospheric aerosols have been carried out at urban,^{23–26} remote,^{27,28} oceanic,^{28–30} and polar sites^{31,32} worldwide, from which it was proposed that industrial emissions, subsequent in-aerosol photoreduction, and conversion of Hg(0) to PBM are crucial factors regulating the variations in PBM isotopic composition.^{27,28,32,33} Oxidation processes were also speculated to be of potential importance in an oceanic study, but the detailed mechanisms remain largely unknown.²⁹ Hence, the links between heterogeneous Hg reactions in aerosols and PBM isotopic signature have yet to be established.

Considering the crucial roles PBM plays in atmospheric Hg cycling,^{7,8,34} further investigation of Hg transformation at the interface of and within aerosols using diversified approaches is warranted.^{7,8} In the present study, we measured the isotopic composition of PBM in 10 Chinese megacities. PBM concentrations in Chinese urban areas are generally highly elevated and represent the major Hg species scavenged from the atmosphere in China.^{35,36} The PBM isotope signatures together with the chemical characteristics of $\text{PM}_{2.5}$ and meteorological parameters were used to explore the effect of in-aerosol Hg transformation on the MIF of PBM. Finally, PBM sourced from atmospheric oxidation of Hg(0) followed by aerosol scavenging processes is constrained using a $\Delta^{200}\text{Hg}$ mixing model.

2. MATERIALS AND METHODS

2.1. PBM Sampling. PBM samples were collected at downtown sites in 10 megacities in China (i.e., Beijing, Shijiazhuang, Jinan, Lanzhou, Zhengzhou, Shanghai, Chengdu, Wuhan, Guiyang, and Guangzhou) (Figure S1). Detailed information on the sampling sites and the cities can be found in Fu et al.³⁷ $\text{PM}_{2.5}$ samples were collected on quartz fiber filters (8×10 in sheet, Munktell, Sweden) using high-volume $\text{PM}_{2.5}$ samplers (ASM-1, Guangzhou Minya, China) at a flow rate of $1.0 \text{ m}^3 \text{ min}^{-1}$. Before sampling, quartz filters were preheated at $500 \text{ }^\circ\text{C}$ for 6 h to minimize the Hg blank in filters. In this study, daily $\text{PM}_{2.5}$ samples were continuously collected for approximately 1 week at each urban site in both summer and winter campaigns (Table S1). Filters were sealed carefully in polyethylene bags immediately after the completion of field sampling and kept frozen ($-18 \text{ }^\circ\text{C}$) before further sample processing.

2.2. Sample Processing and Analysis. A small piece ($\sim 10\%$) of filter was cut off from the large filter sheets (8×10 in.) using a Teflon scissor for the analysis of PBM concentration and isotopic composition. The filters were combusted in a Hg-free oxygen flow in a quartz tube (25 mL

min^{-1}), and then PBM in $\text{PM}_{2.5}$ was thermally released as Hg(0), which was subsequently preconcentrated into 5 mL of 40% HNO_3/HCl mixed trapping solution (v/v, 2:1).³⁸ Hg concentration in the trapping solution was measured using a cold vapor atomic fluorescence spectroscopy method. PBM concentration in ambient air was calculated by dividing the Hg mass in the trapping solution by the sampling air volume through the filter piece.

Isotope ratios of Hg in the trapping solution were determined using cold vapor multicollector inductively coupled plasma mass spectrometry (Nu-Plasma, UK).²⁸ MDF and MIF values of PBM were reported in delta notation (δ) and capital delta (Δ) in per mil (‰), respectively, which were calculated using the following equations³⁹

$$\delta^{\text{xxx}}\text{Hg} = \left[\frac{(\text{xxxHg}/^{198}\text{Hg})_{\text{sample}}}{(\text{xxxHg}/^{198}\text{Hg})_{\text{NIST-3133}}} - 1 \right] \times 1000 \quad (1)$$

$$\Delta^{\text{xxx}}\text{Hg} = \delta^{\text{xxx}}\text{Hg} - \beta \times \delta^{202}\text{Hg} \quad (2)$$

where xxx is the mass number of Hg isotopes (199, 200, 201, 202, and 204), sample is the PBM collected in the present study, NIST-3133 is the bracketing NIST SRM 3133 Hg standard reference during analysis, and β is 0.2520, 0.5024, 0.7520, and 1.493 for ^{199}Hg , ^{200}Hg , ^{201}Hg , and ^{204}Hg , respectively, which are determined from the kinetic MDF law.³⁹

The recoveries of sample processing were investigated by combustions of CRM BCR-482 (lichen), NSIT SRM 2711a (Montana soil), and NIST SRM 1648 (urban particulate matter), which showed mean recoveries of $87.9 \pm 6.6\%$ (1sd, $n = 6$), $96.0 \pm 4.2\%$ (1sd, $n = 6$), and $91.9 \pm 10.8\%$ (1sd, $n = 19$), respectively. The combustion of preheated filters showed a mean system blank of $0.09 \pm 0.05 \text{ ng mL}^{-1}$ (1sd, $n = 15$) for the field sampling and processing, which accounted for <10% of the collected PBM in trap solutions. Isotope ratios of Hg in NIST SRM 3177, SRM 2711a, and BCR 482 were routinely measured during the analysis of the PBM isotopic composition, which agree well with previously reported values (Table S2).^{12,40} The reported analytical uncertainty of the PBM isotopic composition in this study is the higher 2sd value of either NIST SRM 3177 or the repeated analysis of PBM samples.

2.3. Ancillary Parameters. $\text{PM}_{2.5}$ mass concentration, organic carbon (OC), elemental carbon (EC), water-soluble anions (including Cl^{-1}), and trace elements (including Fe and Cd) in $\text{PM}_{2.5}$ samples were analyzed to investigate the effect of environmental factors on the variations of PBM isotopic compositions, and details of the processing and analysis are shown in Text S1.

3. RESULTS AND DISCUSSION

3.1. PBM Concentration and Isotope Composition. City-specific mean PBM concentrations ranged from 33.6 to 158 pg m^{-3} ($n = 10$, Table S3), and the overall mean value from the 10 cities was $74.9 \pm 82.9 \text{ pg m}^{-3}$ (1sd, $n = 130$) during the study period. This mean value was approximately 1.5 times of that obtained from Chinese rural areas and more than 1 order of magnitude higher than those in North America and Europe.^{35,41} The mean concentration of PBM in the cities was not correlated with that of $\text{PM}_{2.5}$ or EC (ANOVA, $p > 0.05$ for both) but significantly positively correlated with that of OC ($r^2 = 0.89$, $p < 0.01$) (Figure S2). The strong correlation

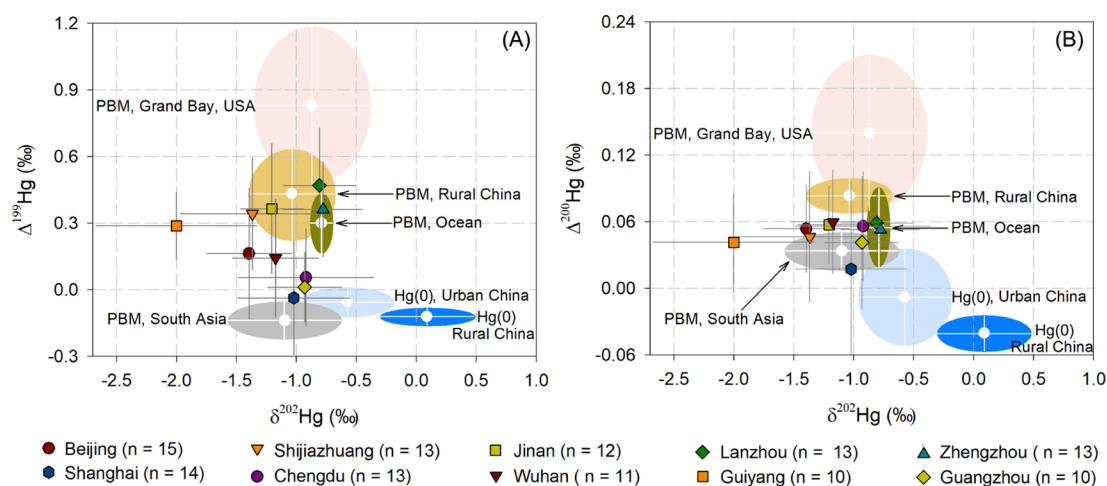


Figure 1. Mean (± 1 sd) of $\delta^{202}\text{Hg}$ vs $\Delta^{199}\text{Hg}$ (A) and $\delta^{202}\text{Hg}$ vs $\Delta^{200}\text{Hg}$ (B) for PBM collected in the 10 megacities in this study. Observations of $\delta^{202}\text{Hg}$, $\Delta^{199}\text{Hg}$, and $\Delta^{200}\text{Hg}$ for PBM in rural areas of China,²⁸ oceans,^{28–30} urban areas of South Asia,^{25,26} and USA,²⁷ as well as Hg(0) (GEM) in urban and rural areas of China^{37,51,52} were also compiled from previous studies. Error bars are 1sd of the mean values.

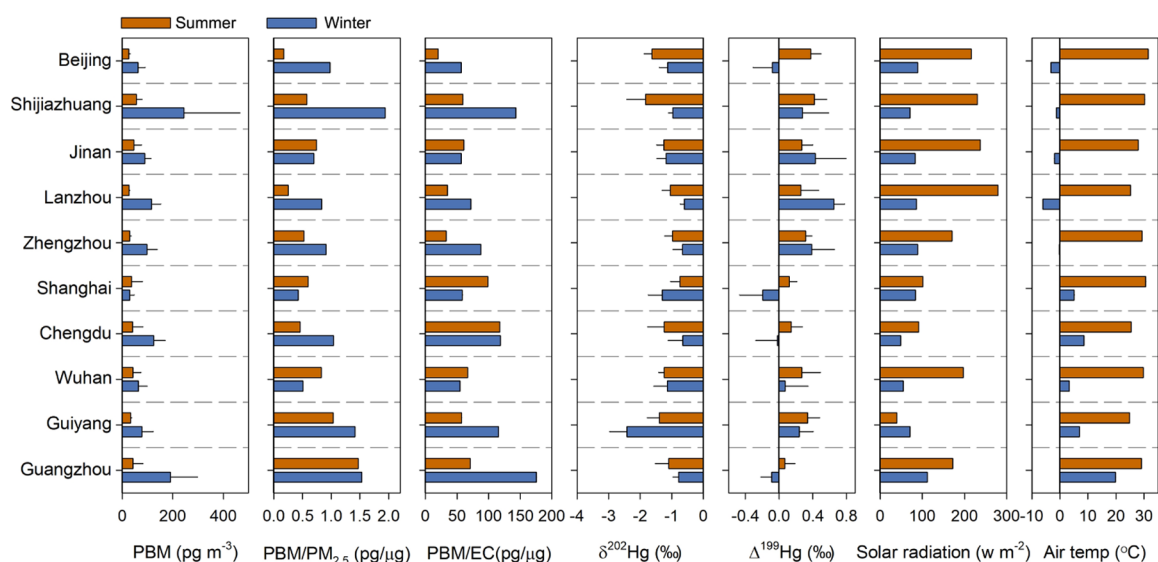


Figure 2. Summertime and wintertime means of PBM concentrations, PBM/PM_{2.5} ratios, PBM/EC ratios, $\delta^{202}\text{Hg}_{\text{PBM}}$, $\Delta^{199}\text{Hg}_{\text{PBM}}$, solar radiation, and air temperature at the 10 urban sites. Error bars are 1sd of the mean values.

between PBM and OC is similar to the observations in precipitation samples.⁴² The high mass fraction of OC in aerosols is conducive to the GOM adsorption by aerosols or aerosol water and the complexation of Hg(II) inside aerosols,^{43,44} which may therefore represent a major factor controlling the PBM variation among the investigated cities.

Isotopic compositions of daily PBM samples collected in the 10 cities exhibited large variations, with $\delta^{202}\text{Hg}$, $\Delta^{199}\text{Hg}$, and $\Delta^{200}\text{Hg}$ values in the range of -3.28 to 0.41‰ , -0.67 to 0.94‰ , and -0.13 to 0.16‰ ($n = 125$), respectively (Table S1). A minor fraction of PBM samples (16% of the total collected samples) were characterized by negative $\Delta^{199}\text{Hg}$ values, which were mainly observed in the winter campaign (Table S1). City-specific mean $\delta^{202}\text{Hg}$, $\Delta^{199}\text{Hg}$, and $\Delta^{200}\text{Hg}$ values of PBM during the study period ranged from -2.00 to -0.78 , -0.04 to 0.47 , and 0.02 to 0.06‰ ($n = 10$), respectively, while the overall mean from all the 10 cities were -1.16 , 0.22 , and 0.05‰ , respectively (Figure 1 and Table S3). PBM isotopic compositions observed in the present study align well with the pool of global PBM data, which are

characterized by significantly negative $\delta^{202}\text{Hg}$ (mean = -1.64 to -0.69‰), slightly negative to significantly positive $\Delta^{199}\text{Hg}$ (mean = -0.21 to 0.83‰), and positive $\Delta^{200}\text{Hg}$ (mean: 0.01 to 0.14‰) signatures (Table S3),^{23–30,45,46} with the exception of the observations in polar regions (mean $\delta^{202}\text{Hg} = 0.03$ to 1.05‰ , mean $\Delta^{199}\text{Hg} = -0.38$ to -0.28‰ , mean $\Delta^{200}\text{Hg} = -0.01$ to 0.00‰ , $n = 2$) (Table S3).^{31,32} By comparison, PBM at urban sites worldwide showed relatively lower $\Delta^{199}\text{Hg}$ and $\Delta^{200}\text{Hg}$ values as compared to observations at Chinese rural sites, in marine air, and at a coastal site in the United States (Figure 1). The isotopic composition in flue gases and other primary anthropogenic emissions shows slightly negative to near-zero values of $\Delta^{199}\text{Hg}$ and $\Delta^{200}\text{Hg}$.^{47–49} The lower values of PBM $\Delta^{199}\text{Hg}$ and $\Delta^{200}\text{Hg}$ at urban sites would therefore suggest relatively higher contributions from primary anthropogenic emissions (PBM emissions and adsorption of GOM emitted from anthropogenic sources) to PBM in the urban areas.^{34,50}

The isotopic compositions of PBM in this and previous studies are generally distinguishable from those of Hg(0) and

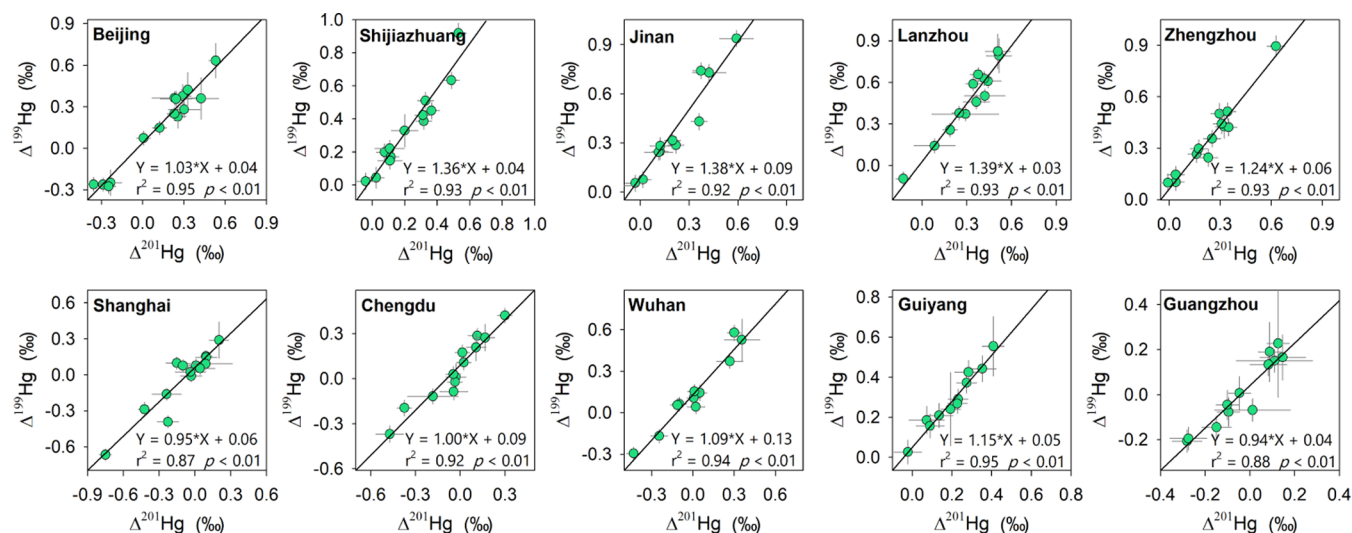


Figure 3. Linear regression analysis (variables entered—SPSS Statistics) between $\Delta^{199}\text{Hg}$ and $\Delta^{201}\text{Hg}$ of daily PBM samples in the 10 cities.

GOM (Figure 1 and Table S3). For example, the isotopic composition of Hg(0) at urban and rural sites in China showed relatively lower $\Delta^{199}\text{Hg}$ (mean_{urban} = $-0.06 \pm 0.06\%$, mean_{rural} = $-0.12 \pm 0.04\%$) and $\Delta^{200}\text{Hg}$ (mean_{urban} = $-0.01 \pm 0.04\%$, mean_{rural} = $-0.04 \pm 0.02\%$) values.^{37,45,51,52} Mean $\Delta^{199}\text{Hg}$ and $\Delta^{200}\text{Hg}$ values of GOM at Grand Bay, United States, and Pic Du Midi, France, ranged from -0.11 to 0.44 and 0.15 to 0.18% , respectively.^{22,27} The mechanisms underlying the discernible MIF signatures among atmospheric Hg species, although not well constrained, were proposed to be mainly associated with photochemical reactions in the atmosphere.^{19,20,22,28,33}

3.2. Seasonal Variations in PBM Concentration and Isotope Composition. City-specific mean PBM concentrations in winter (62.7 to 245 pg m^{-3}) were 1.5 to 4.5 times of those (25.3 to 56.7 pg m^{-3}) in summer in nine cities and were 20% lower in one city (Shanghai) during the study period (Figure 2). Such a seasonal variation in PBM concentration (i.e., higher level in winter than in summer) is consistent with those previously reported for urban and rural locations in Mainland China.³⁵ The mean PBM/PM_{2.5} ratio and PBM/EC ratio in the 10 cities were also higher in winter (PBM/PM_{2.5} = $1.03 \pm 0.48 \text{ pg m}^{-3}/\mu\text{g m}^{-3}$, PBM/EC = $94.1 \pm 42.6 \text{ pg m}^{-3}/\mu\text{g m}^{-3}$) than in summer (PBM/PM_{2.5} = $0.67 \pm 0.38 \text{ pg m}^{-3}/\mu\text{g m}^{-3}$, PBM/EC = $62.0 \pm 29.8 \text{ pg m}^{-3}/\mu\text{g m}^{-3}$) (Figure 2). These observations indicate an enrichment of Hg in atmospheric particles in winter, likely due to the increase in the gas-particle partitioning of GOM, decrease in the photochemical losses of Hg from particles under cold and darker conditions, and/or change in the anthropogenic emission sources (Figure 2).^{3,34,50}

During the study period, city-specific mean PBM $\delta^{202}\text{Hg}$ values ranged from -1.83 to -0.74% (mean = -1.24% , $n = 10$) in summer, which were lower than the corresponding values in winter in most cities except in Shanghai and Guiyang (from -2.42 to -0.60% , mean = -1.08% , $n = 10$) (Figure 2). Mean PBM $\Delta^{199}\text{Hg}$ values in summer (0.07 to 0.42%) were higher than the corresponding observations in winter (-0.19 to 0.28%) at seven urban sites (Figure 2). A previous study that investigated diel PBM isotopic compositions in Beijing, China, suggested that stronger solar radiation would increase $\Delta^{199}\text{Hg}$ because of the increase in photoreduction

processes.³³ Such a hypothesis could partially explain the relatively higher PBM $\Delta^{199}\text{Hg}$ in summer in the seven cities mentioned above. However, the opposite seasonal pattern was observed in three cities (Jinan, Lanzhou, and Zhengzhou) with higher PBM $\Delta^{199}\text{Hg}$ and much weaker solar radiation intensity in winter than in summer (Figure 2), indicating that other atmospheric reactions likely also played important roles in shaping the MIF of PBM in urban areas (more discussion in Section 3.3).

The relationships between $\Delta^{199}\text{Hg}$ and PBM/PM_{2.5}, PBM/EC, and PBM/Cd ratios were analyzed for revealing the potential transformation mechanism of PBM. EC and Cd in the atmosphere are mainly derived from anthropogenic sources, and Cd shares approximately 80% of the anthropogenic sources for Hg.^{53,54} Therefore, decreasing PBM/PM_{2.5}, PBM/EC, and PBM/Cd ratios would indicate potential losses of Hg from aerosols due to photoreduction and volatilization processes. PBM $\Delta^{199}\text{Hg}$ significantly negatively correlated with PBM/EC and PBM/Cd ratios (ANOVA, $r^2 = 0.45$ to 0.59 , $p < 0.05$) in summer but only weakly and insignificantly negatively correlated with PBM/PM_{2.5} ($r^2 = 0.19$, $p = 0.21$) (Figure S3). The PBM samples collected in summer ($n = 56$) displayed a $\Delta^{199}\text{Hg}/\Delta^{201}\text{Hg}$ slope of 1.04 (Figure S4), which was within the range of those (1.00 to 1.12) derived from the photoreduction of Hg(II) complexed with dissolved organic carbon (DOC) and soot particles and anthropogenic sources.^{11,55,56} These findings suggest that the photoreduction of PBM was likely responsible for the positive $\Delta^{199}\text{Hg}$ values in summer in these cities. In contrast, no significant correlations were observed between PBM $\Delta^{199}\text{Hg}$ and PBM/PM_{2.5}, PBM/EC, and PBM/Cd ratios in winter, and the $\Delta^{199}\text{Hg}/\Delta^{201}\text{Hg}$ slope was 1.20 (Figures S3 and S4). We reason that the partitioning of GOM to PBM increases during winter, and this addition of Hg(II) is then processed to a greater extent by reactions within aerosols (more discussion in Section 3.3).^{7,34}

3.3. Odd-Hg MIF Induced by Mercury Transformations in Aerosols. PBM in the atmosphere is mainly derived from primary anthropogenic emissions and gas-particle partitioning of GOM,^{8,34,50} whereas the adsorption and oxidation of Hg(0) on aerosol surfaces are generally considered less relevant due to its low solubility in liquid

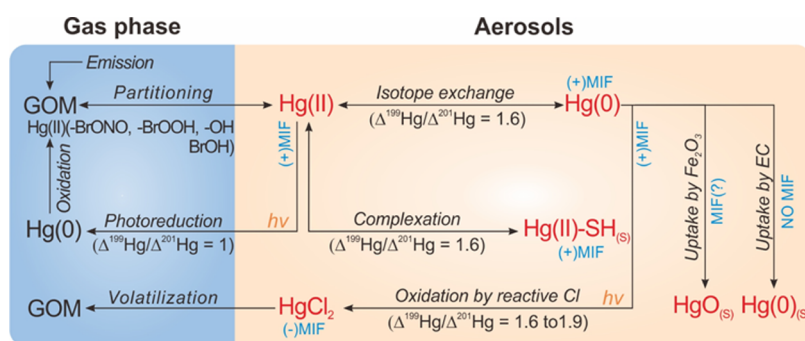


Figure 4. Diagram scheme showing the odd-MIF of PBM isotopes caused by potential physicochemical reactions in aerosols. GOM compounds produced from gaseous-phase Hg(0) oxidation are from previous studies.^{4,8} Photoreduction of Hg(II) in aerosols is expected to generate a $\Delta^{199}\text{Hg}/\Delta^{201}\text{Hg}$ ratio of ~ 1.0 and positive odd-MIF in reactant Hg(II) due to (+)MIE.^{11,55,56,61} We speculate that diagnostic $\Delta^{199}\text{Hg}/\Delta^{201}\text{Hg}$ ratios higher than 1.0 were caused by other heterogeneous Hg reactions in aerosols [e.g., complexation of Hg(II) with thiol (–SH), Hg(II)–Hg(0) isotope exchange, aqueous photooxidation of Hg(0) by reactive chloride] that express NVE.^{12,16,18,71}

aerosols,⁵⁷ low uptake by soot,⁵⁸ and weak reactivity at the interface.⁵⁹ The MIF of Hg isotopes and $\Delta^{199}\text{Hg}/\Delta^{201}\text{Hg}$ ratios can be potential tracers of Hg transformations. In the present study, we observed that city-specific mean $\Delta^{199}\text{Hg}/\Delta^{201}\text{Hg}$ ratios of PBM varied noticeably from 0.94 ± 0.12 to 1.39 ± 0.11 (Figure 3), and the mean $\Delta^{199}\text{Hg}$ of PBM increased linearly with this ratio (ANOVA, $r^2 = 0.90$, $p < 0.01$, Figure S5).

The much higher than unity $\Delta^{199}\text{Hg}/\Delta^{201}\text{Hg}$ ratios of PBM observed in some cities (e.g., 1.24 to 1.39 in Shijiazhuang, Jinan, Lanzhou, and Zhengzhou) were not likely inherited from GOM during gas-particle partitioning because the available global data showed $\Delta^{199}\text{Hg}/\Delta^{201}\text{Hg}$ ratios of GOM of around 1.0.^{22,27} Global source materials and anthropogenic PBM emissions generally have a small magnitude of odd-MIF and a $\Delta^{199}\text{Hg}/\Delta^{201}\text{Hg}$ ratio of ~ 1.0 ⁶⁰ and therefore should not be the cause of the observed high $\Delta^{199}\text{Hg}/\Delta^{201}\text{Hg}$ ratios. Generally, large MIF of odd-Hg isotopes is mainly induced by the MIE during photochemical redox reactions of Hg in the environment. Photoreduction of Hg(II) may result in either (+)MIE (positive $\Delta^{199}\text{Hg}$ in the reactant) or (–)MIE (negative $\Delta^{199}\text{Hg}$ in the reactant), depending on the complexes of Hg(II) and reaction conditions.^{15,55,61} Experimental studies on the photoreduction of Hg(II) in water (DOC complexed), water-saturated soot particles, and soil show (+)MIE with $\Delta^{199}\text{Hg}/\Delta^{201}\text{Hg}$ ratios ranging from 1.0 to 1.12,^{11,55,56,61,62} and this explains well the $\Delta^{199}\text{Hg}/\Delta^{201}\text{Hg}$ ratios (0.94 to 1.15) observed in 6 out of the 10 cities (Figure 3). The photoreduction of Hg(II) complexed with S-containing ligands can potentially generate high $\Delta^{199}\text{Hg}/\Delta^{201}\text{Hg}$ ratios of up to 1.34 to 1.46 accompanied by significantly negative $\Delta^{199}\text{Hg}$ in reactant Hg(II) due to (–)MIE.^{55,61} The photochemical gas-phase oxidation of Hg(0) by atomic Br and Cl has $\Delta^{199}\text{Hg}/\Delta^{201}\text{Hg}$ ratios of 1.64 and 1.89, respectively, but would likely result in negative $\Delta^{199}\text{Hg}$ in PBM following the adsorption of the GOM reaction product by particles.¹² These experimental results are in contrast, at least to a certain extent, with the observations in Shijiazhuang, Jinan, Lanzhou, and Zhengzhou (e.g., high $\Delta^{199}\text{Hg}/\Delta^{201}\text{Hg}$ ratios of 1.24 to 1.39 and highly positive mean $\Delta^{199}\text{Hg}$ of 0.34 to 0.47‰, Figure 3). A previous study showed that the $\Delta^{199}\text{Hg}/\Delta^{201}\text{Hg}$ ratio increased from 1.19 to 1.31 with the increase in the Hg/DOC ratio from 34.6 to 8330 ng/mg during aqueous Hg(II) photoreduction.¹³ Given the fractions (mean: 67%) of water-soluble OC in total OC in

aerosols,⁶³ we estimated that the mean water-soluble Hg/DOC ratio in aerosols would not exceed 24 ng/mg in these cities (Table S1), which corresponds to the lowest Hg/DOC experiments in the previous study.¹³ Thus, the Hg/DOC ratio was likely not the control factor for the observed high $\Delta^{199}\text{Hg}/\Delta^{201}\text{Hg}$ ratios in some cities. MIF of Hg isotopes during dark abiotic Hg(II) reduction dominated by NVE is characterized by a $\Delta^{199}\text{Hg}/\Delta^{201}\text{Hg}$ ratio of ~ 1.6 .^{13,17} This process, however, is expected to play a minor role because of its fairly slow reaction rates in solutions and aerosols and negative $\Delta^{199}\text{Hg}$ signatures in reactant Hg(II).^{13,64}

In the present study, we found the $\Delta^{199}\text{Hg}/\Delta^{201}\text{Hg}$ ratio in the 10 cities negatively correlated with air temperature (ANOVA, $r^2 = 0.66$, $p < 0.01$) and positively correlated with water-soluble Cl^- , total Fe, and EC concentrations in aerosols (ANOVA, $r^2 = 0.54$ to 0.64 , $p < 0.01$ or 0.05) (Figure S6). Low air temperatures enhance the gas-particle partitioning of GOM,³⁴ high levels of Cl^- promote Hg(0) oxidation,⁶⁵ and high Fe (partial in the Fe_2O_3 form) and EC (S-rich) contents facilitate the uptake of Hg(0) in aerosols.^{66,67} These factors can together facilitate the physicochemical reactions of Hg compounds in aerosols following the strong gas-particle partitioning of GOM. Recent modeling studies have suggested that the major Hg(II) products derived from atmospheric Hg(0) gas-phase oxidation are mainly complexed with $-\text{BrONO}$, $-\text{BrOOH}$, $-\text{BrOH}$, and $-\text{OH}$,^{4,8} whereas Hg compounds in airborne particles are expected to include Hg(0), Hg(I), HgCl₂, HgS, and HgO.^{68,69} We therefore hypothesize that substantial physicochemical transformations of Hg compounds may exist in aerosols following the gas-particle partitioning of GOM. This hypothesis is used here to interpret the odd-MIF of PBM (Figure 4).

Following the partitioning of GOM [Hg(II)] into aerosols, Hg(II) can partition back to the gas phase directly or after complexation and respeciation^{8,34} and undergo photoreduction to form Hg(0), which is either released back to the atmosphere or retained in aerosols. The photoreduction of Hg(II) is expected to drive a large positive $\Delta^{199}\text{Hg}$ shift and generate a $\Delta^{199}\text{Hg}/\Delta^{201}\text{Hg}$ ratio of ~ 1.0 in reactant Hg(II) in aerosols due to (+)MIE.^{11,55,61} In addition to Hg(II) photoreduction, a fraction of Hg(II) is likely complexed with thiol functional groups, and this equilibrium process results in a small positive $\Delta^{199}\text{Hg}$ shift (e.g., $< 0.1\%$) in thiol-bound Hg(II) relative to reactant Hg(II) and a $\Delta^{199}\text{Hg}/\Delta^{201}\text{Hg}$ ratio of ~ 1.6 due to NVE.¹⁶ The thiol-bound Hg(II) displays a limited reactivity

toward photoreduction and therefore tends to be retained in aerosols.⁷⁰ More importantly, we propose that the redox reactions involving Hg compounds in aerosols are also crucial for the odd-MIF of PBM (Figure 4). Once reduced, Hg(0) in aerosols may be rapidly re-oxidized back to Hg(II), especially in the presence of abundant Cl⁻ [through the production of reactive chlorine species or complex Hg(II) product], trace metals in higher oxidation states (e.g., Fe₂O₃), and organic and humic acid, as observed in previous studies.^{18,63,67} The coexistence of Hg(0) and Hg(II) in aerosols facilitates the Hg(0)–Hg(II) isotope exchange, which in turn generates a $\Delta^{199}\text{Hg}/\Delta^{201}\text{Hg}$ ratio of ~ 1.6 due to NVE and a positive $\Delta^{199}\text{Hg}$ shift (up to 0.18‰) in Hg(0) retained in aerosols.¹⁸ In addition, reactive chloride readily oxidizes Hg(0) in liquid aerosols (triggered by OH and/or ozone),⁶⁷ which has been observed to produce large MIF of odd-Hg isotopes ($E^{199}\text{Hg}_{\text{reactant-product}} = 0.13$ to 0.44‰) and $\Delta^{199}\text{Hg}/\Delta^{201}\text{Hg}$ ratios of 1.6 to 1.9 by gas-phase and aqueous experiments.^{12,71} As highlighted by a recent modeling study,⁸ a substantial fraction of photostable HgCl₂ (negative $\Delta^{199}\text{Hg}$) produced in this manner would be partitioned into the gas phase, which in turn leads to an increase in the $\Delta^{199}\text{Hg}$ and $\Delta^{199}\text{Hg}/\Delta^{201}\text{Hg}$ ratio in the aerosol Hg pool. The remaining fractions of Hg(0) could be retained in aerosols by adsorption to EC soot and Fe₂O₃ nanoparticles,^{68,72,73} preserving the positive MIF signatures of Hg(0) in aerosols (Figure 4). The above hypothesis is supported by the observed effects of water-soluble Cl⁻, total Fe, and EC in aerosols on the variations in the $\Delta^{199}\text{Hg}/\Delta^{201}\text{Hg}$ ratio (Figure S6). These factors together facilitate the physicochemical reactions of Hg compounds in aerosols [e.g., Hg(II) thiol complexation, reactive chloride oxidation, and nanoparticle uptake of Hg(0)], which potentially lead to positive shifts of odd-Hg MIF and increased $\Delta^{199}\text{Hg}/\Delta^{201}\text{Hg}$ ratio in PBM. Based on a binary mixing model of NVE and MIE fractionation and their respective typical $\Delta^{199}\text{Hg}/\Delta^{201}\text{Hg}$ ratios of 1.6 and 1.0 (Text S2 and Figure S7), we roughly estimate that the shifts in PBM $\Delta^{199}\text{Hg}$ due to the NVE in Shijiazhuang, Jinan, Lanzhou, and Zhengzhou were on average 0.26‰ (0.00 to 0.55‰), 0.31‰ (0.00 to 0.70‰), 0.46‰ (0.00 to 0.67‰), and 0.16‰ (0.00 to 0.41‰), respectively. These values were somewhat higher than those produced during Hg(II) thiol complexation and Hg(0)–Hg(II) isotope exchange experiments ($\Delta^{199}\text{Hg} < 0.2\%$)^{16,18} but within the range of those produced during Cl-triggered Hg(0) oxidation ($\Delta^{199}\text{Hg}$ up to $\sim 1.2\%$).^{12,71} We caution that several Hg(II) photoreduction experiments have reported $\Delta^{199}\text{Hg}/\Delta^{201}\text{Hg}$ ratios of higher than 1.0 for (+)MIE,^{13,61} and a use of a $\Delta^{199}\text{Hg}/\Delta^{201}\text{Hg}$ ratio of 1.19 for (+)MIE that resembles the Hg/DOC ratio in aqueous aerosols in this study would predict smaller contributions of NVE to the odd-Hg MIF in these cities (Text S2).¹³ Nevertheless, higher $\Delta^{199}\text{Hg}/\Delta^{201}\text{Hg}$ ratios (e.g., 1.24 to 1.39) in the present study than photoreduction experiments suggest that photochemical Hg(II) reduction should not be the exclusive origin of the odd-Hg MIF in aerosols, and other in-aerosol heterogeneous Hg reactions should be also considered to interpret the odd-MIF signatures of PBM in the urban environment.

3.4. PBM Originating from Atmospheric Hg(0) Oxidation. Recent studies have explored the MIF variability of even-Hg isotopes (e.g., $\Delta^{200}\text{Hg}$), which is thought to be produced during photochemical Hg redox reactions at high altitudes and distinguishable among atmospheric Hg species [e.g., $\Delta^{200}\text{Hg}$ of Hg(0) vs GOM and wet deposition].^{12,20,22,74}

$\Delta^{200}\text{Hg}$ has been used to track the pathways of atmospheric Hg deposition to Earth surface reservoirs.^{21,22,75,76} City-specific mean PBM $\Delta^{200}\text{Hg}$ obtained in the present study ranged from 0.02 to 0.06‰, while higher values (0.01 to 0.14‰) have been reported from rural areas in China ($n = 3$), a coastal site in the United States, and over oceans (Figure 5).^{27–30} PBM in the

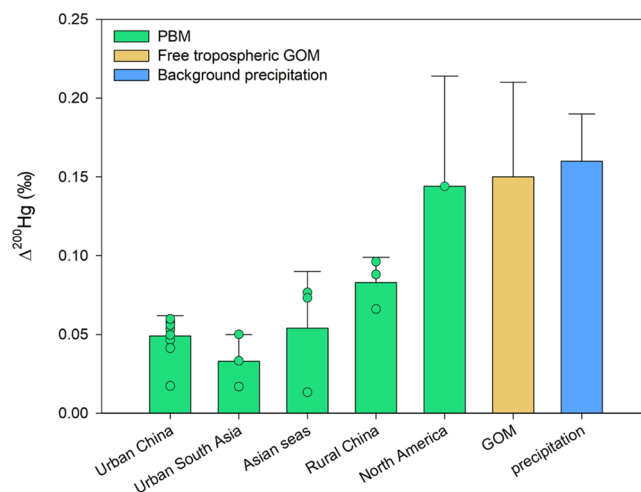


Figure 5. Summary of mean ($\pm 1\text{sd}$) $\Delta^{200}\text{Hg}$ values of PBM, free tropospheric GOM, and background precipitation in different regions worldwide. Data are from this study and the literature.^{22,25–30,76} Green circles indicate the mean PBM $\Delta^{200}\text{Hg}$ values at individual sites ($n = 20$).

atmosphere is sourced from primary anthropogenic PBM emissions, gas-particle partitioning of GOM emitted from anthropogenic sources, and gas-particle partitioning of GOM produced during atmospheric Hg(0) oxidation. PBM and GOM directly emitted from anthropogenic sources are expected to have $\Delta^{200}\text{Hg}$ values around $0.00 \pm 0.03\%$.^{60,77} The positive shift in the observed $\Delta^{200}\text{Hg}_{\text{PBM}}$ (higher values than $\sim 0.00\%$ mentioned above) could be mainly caused by gas-particle partitioning of GOM produced by Hg(0) oxidation, which is observed to carry significantly positive $\Delta^{200}\text{Hg}$ values.^{22,27} Here we use $\Delta^{200}\text{Hg}$ to estimate the fraction of PBM sourced from atmospheric Hg(0) oxidation ($F_{\text{Hg(0)-oxidation}}$) based on eqs 3 and 4.

$$\Delta^{200}\text{Hg}_{\text{sample}} = F_{\text{anthropogenic}} \times \Delta^{200}\text{H} \quad (3)$$

$$\begin{aligned} & \times \left(F_{\text{PBM \& GOM-anthropogenic}} + F_{\text{Hg(0)-oxidation}} \right) \\ & \times \Delta^{200}\text{Hg}_{\text{Hg(0)-oxidation}} \end{aligned}$$

$$F_{\text{anthropogenic}} + F_{\text{Hg(0)-oxidation}} = 1 \quad (4)$$

where $\Delta^{200}\text{Hg}_{\text{sample}}$ is the observed $\Delta^{200}\text{Hg}$ values of PBM samples, $\Delta^{200}\text{Hg}_{\text{PBM\&GOM-anthropogenic}}$ is the $\Delta^{200}\text{Hg}$ values of anthropogenic emitted PBM and GOM, $\Delta^{200}\text{Hg}_{\text{Hg(0)-oxidation}}$ is the $\Delta^{200}\text{Hg}$ signature of GOM produced by Hg(0) oxidation, and $F_{\text{anthropogenic}}$ and $F_{\text{Hg(0)-oxidation}}$ are the fractions of PBM derived from anthropogenic emissions (PBM and gas-particle partitioning of GOM emitted from anthropogenic sources) and gaseous Hg(0) oxidation followed by gas-particle partitioning of GOM, respectively.

The $\Delta^{200}\text{Hg}$ signature of GOM produced by Hg(0) oxidation ($\Delta^{200}\text{Hg}_{\text{Hg(0)-oxidation}}$) is estimated to be $0.15 \pm 0.06\%$ based on observations in the free troposphere,²² and

this value is close to the mean $\Delta^{200}\text{Hg}$ of precipitation at global background sites (0.16‰),⁷⁶ which dominantly originated from the removal of GOM produced in the free troposphere.^{3,78} Figure 5 shows the mean $\Delta^{200}\text{Hg}$ values of PBM, GOM, and precipitation at global sites excluding the polar region, where the near-zero $\Delta^{200}\text{Hg}$ values of PBM are due to insufficient understanding of transformation mechanisms.^{31,32} Hence, the mean fractions ($\pm 1\text{sd}$) of PBM sourced from atmospheric Hg(0) oxidation followed by gas-particle partitioning of GOM were estimated to be 42 ± 25 , 35 ± 24 , 52 ± 26 , 46 ± 26 , and $60 \pm 25\%$ in urban China, urban South Asia, rural China, Asian seas, and North American, respectively, using Monte Carlo simulation (Text S3 and Figures S8 and S9). A combination of the above results yields a mean fraction ($\pm 1\text{sd}$) of $47 \pm 22\%$ for the PBM sourced from atmospheric Hg(0) oxidation. This, together with the dominant contribution of Hg(0) oxidation to PBM in the polar region,³² suggests that PBM is potentially an important sink for Hg(0) in the global atmosphere. For example, given the contributions of atmospheric Hg(0) oxidation to PBM and a total PBM deposition of 229 tons/year in China,³⁶ we estimated that approximately 108 tons of Hg(0) in the atmosphere in China are removed annually via transformation to PBM, which accounts for 36% of the anthropogenic Hg(0) emissions in China.⁵⁰

4. ENVIRONMENTAL IMPLICATIONS

Aerosols play a crucial role in the biogeochemical cycling of Hg in the atmosphere,^{3,8} but the knowledge concerning Hg chemistry in aerosols is limited.⁷ PBM has been observed to frequently carry significantly positive $\Delta^{199}\text{Hg}$ values, which are clearly different from the corresponding signature for primary anthropogenic emissions.^{23,27,28} Positive $\Delta^{199}\text{Hg}_{\text{PBM}}$ signatures together with a $\Delta^{199}\text{Hg}_{\text{PBM}}/\Delta^{201}\text{Hg}_{\text{PBM}}$ ratio of ~ 1.0 reported in previous studies indicate that the photoreduction of Hg(II) occurred in aerosols,^{24,27,28,33} which is generally accounted for in modeling studies.^{3,8} In the present study, we found that the $\Delta^{199}\text{Hg}_{\text{PBM}}/\Delta^{201}\text{Hg}_{\text{PBM}}$ ratio varied largely from 0.94 to 1.39 in 10 Chinese megacities and the ratio increased with the mean $\Delta^{199}\text{Hg}_{\text{PBM}}$ value in any individual city during the study period. We speculated that other reaction processes, including isotope exchange between Hg(II) and Hg(0), Hg(II) complexation with thiols, and photochemical oxidation of Hg(0) by reactive chloride in aerosols, are also potential factors influencing the odd-MIF of PBM in the present study. This is especially the case in the urban atmosphere with elevated aerosol contents of chloride, Fe, and EC. This hypothesis could potentially explain the observed compounds of Hg in PBM⁶⁸ and the most abundant gaseous HgCl_2 compound simulated in the atmosphere.⁸ Mercury chemistry in aerosols likely produces Hg compounds with different photochemical behaviors than those produced via gas-phase chemistry,^{4,8,70} which therefore has a potential to influence the photochemistry of atmospheric Hg. It should be noted that the diagnostic $\Delta^{199}\text{Hg}_{\text{PBM}}/\Delta^{201}\text{Hg}_{\text{PBM}}$ ratios at many sites in this and previous studies resemble those of Hg(II) photoreduction,^{23,24,27,28} indicating that the photoreduction of Hg(II) is likely the dominant mechanism inducing the positive PBM MIF in the continental atmosphere. It seems to be plausible that the Hg transformation in aerosols is largely influenced by aerosol chemistry and meteorological parameters, and the PBM isotope signatures imparted by these processes would differ noticeably over different time scales and in various atmospheric

environments. The samples in the present study were collected during short sampling periods, and it is therefore not clear whether the proposed reaction processes in this study would be environmentally relevant for the aerosols in the global atmosphere. In addition, high $\Delta^{199}\text{Hg}/\Delta^{201}\text{Hg}$ ratios in the present study were accompanied by low air temperature and elevated aerosol contents of chloride, Fe, and EC. Previous studies found that the odd-MIF during photoreduction could be affected by Hg(II) complexation to organic ligands, pH, and dissolved oxygen levels,^{55,61} whereas the effects of temperature, halogens (e.g., Cl and Br), Fe, and EC on the odd-MIF during aqueous/in-aerosol photochemical and non-photochemical reactions are not well understood. Further studies on PBM isotope signatures in various atmospheric environments and fractionation of stable Hg isotope during heterogeneous Hg reactions in aerosols under various environmental conditions are needed to improve our knowledge of the physicochemical reactions of Hg in aerosols.

There is an increasing consensus that Hg(0) in the atmosphere is more readily deposited to the Earth surface reservoir than traditionally assumed;^{75,76,79,80} however, missing atmospheric Hg oxidation processes may still exist in light of the fast photolysis of major constituents of gaseous oxidized Hg.⁹ Based on the $\Delta^{200}\text{Hg}$ signatures of speciated atmospheric Hg, we estimate that an important fraction of PBM ($47 \pm 22\%$ on global average) is sourced from Hg(0) oxidation followed by the partitioning of GOM into aerosols. Previous studies have revealed that gas-particle partitioning of GOM, which is from both anthropogenic emission and Hg(0) oxidation, is an important source of PBM,³⁴ while the present study for the first time quantified the fraction of PBM sourced from the atmospheric Hg(0) oxidation process. We caution that, due to the insufficient knowledge of the even-MIF mechanisms and signatures associated with atmospheric Hg, our estimate would have large uncertainties. In the present study, we assume that the observations of GOM $\Delta^{200}\text{Hg}$ in the free troposphere is representative of the $\Delta^{200}\text{Hg}$ signature of GOM produced by Hg(0) oxidation throughout the troposphere, and Hg reactions in aerosols would not likely produce detectable even-MIF.²² This is because Hg(0) oxidation is thought to mostly occur in the free troposphere, and even-MIF is mainly related to this process.^{3,20,22} However, a recent study suggests that the oxidation of Hg(0) in the marine boundary layer (MBL) should also be important,⁸ and it is unclear whether the $\Delta^{200}\text{Hg}$ signature of GOM produced in the MBL is close to that produced in the free troposphere. In addition, although many experimental studies did not observe detectable even-MIF during the photoreduction of Hg(II) in water, soot particles, and soil,^{11,55,56,61,62} the even-MIF associated with heterogeneous Hg reactions in aerosols remains poorly constrained. Therefore, further field and experimental studies on the MIF of Hg isotopes during atmospheric Hg reactions are still needed in order to better constrain the physicochemical processes and sources of atmospheric Hg.

■ ASSOCIATED CONTENT

Supporting Information

The Supporting Information is available free of charge at <https://pubs.acs.org/doi/10.1021/acs.est.1c08065>.

Additional information about the ancillary methodology, sampling locations, isotopic compositions of PBM, and

relationship analysis between PBM isotopic compositions and ancillary parameters (PDF)

AUTHOR INFORMATION

Corresponding Author

Xuewu Fu – State Key Laboratory of Environmental Geochemistry, Institute of Geochemistry, Chinese Academy of Sciences, Guiyang 550081, China; orcid.org/0000-0002-5174-7150; Email: fuxuewu@mail.gyig.ac.cn

Authors

Chen Liu – State Key Laboratory of Environmental Geochemistry, Institute of Geochemistry, Chinese Academy of Sciences, Guiyang 550081, China; University of Chinese Academy of Sciences, Beijing 100049, China

Yue Xu – State Key Laboratory of Environmental Geochemistry, Institute of Geochemistry, Chinese Academy of Sciences, Guiyang 550081, China

Hui Zhang – State Key Laboratory of Environmental Geochemistry, Institute of Geochemistry, Chinese Academy of Sciences, Guiyang 550081, China; University of Chinese Academy of Sciences, Beijing 100049, China

Xian Wu – State Key Laboratory of Environmental Geochemistry, Institute of Geochemistry, Chinese Academy of Sciences, Guiyang 550081, China; University of Chinese Academy of Sciences, Beijing 100049, China

Jonas Sommar – State Key Laboratory of Environmental Geochemistry, Institute of Geochemistry, Chinese Academy of Sciences, Guiyang 550081, China; orcid.org/0000-0001-8634-440X

Leiming Zhang – Air Quality Research Division, Science and Technology Branch, Environment and Climate Change Canada, Toronto M3H 5T4 Ontario, Canada

Xun Wang – State Key Laboratory of Environmental Geochemistry, Institute of Geochemistry, Chinese Academy of Sciences, Guiyang 550081, China; orcid.org/0000-0002-7407-8965

Xinbin Feng – State Key Laboratory of Environmental Geochemistry, Institute of Geochemistry, Chinese Academy of Sciences, Guiyang 550081, China; University of Chinese Academy of Sciences, Beijing 100049, China; orcid.org/0000-0002-7462-8998

Complete contact information is available at: <https://pubs.acs.org/10.1021/acs.est.1c08065>

Notes

The authors declare no competing financial interest.

ACKNOWLEDGMENTS

This work was supported by the National Key R&D Program of China (2017YFC0212001), the Key Research Program of Frontier Science, Chinese Academy of Sciences (ZDBS-LY-DQC029), the National Nature Science Foundation of China (41921004), and the K. C. Wong Education Foundation. We thank the following research groups for providing assistance in PBM sampling in their respective cities: Prof. Gan Zhang from Guangzhou Institute of Geochemistry, CAS, Guangzhou, China; Prof. Hai Guo from the Hong Kong Polytechnic University, Hong Kong, China; and Prof. Hong Gao from Lanzhou University, Lanzhou, China.

REFERENCES

- (1) Gustin, M.; Jaffe, D. Reducing the Uncertainty in Measurement and Understanding of Mercury in the Atmosphere. *Environ. Sci. Technol.* **2010**, *44*, 2222–2227.
- (2) Holmes, C. D.; Jacob, D. J.; Corbitt, E. S.; Mao, J.; Yang, X.; Talbot, R.; Slemr, F. Global atmospheric model for mercury including oxidation by bromine atoms. *Atmos. Chem. Phys.* **2010**, *10*, 12037–12057.
- (3) Horowitz, H. M.; Jacob, D. J.; Zhang, Y.; Dibble, T. S.; Slemr, F.; Amos, H. M.; Schmidt, J. A.; Corbitt, E. S.; Marais, E. A.; Sunderland, E. M. A new mechanism for atmospheric mercury redox chemistry: implications for the global mercury budget. *Atmos. Chem. Phys.* **2017**, *17*, 6353–6371.
- (4) Saiz-Lopez, A.; Sitkiewicz, S. P.; Roca-Sanjuán, D.; Oliva-Enrich, J. M.; Dávalos, J. Z.; Notario, R.; Jiskra, M.; Xu, Y.; Wang, F.; Thackray, C. P.; Sunderland, E. M.; Jacob, D. J.; Travníkov, O.; Cuevas, C. A.; Acuna, A. U.; Acuña, D.; Plane, J. M. C.; Kinnison, D. E.; Sonke, J. E. Photoreduction of gaseous oxidized mercury changes global atmospheric mercury speciation, transport and deposition. *Nat. Commun.* **2018**, *9*, 4796.
- (5) Obrist, D.; Tas, E.; Peleg, M.; Matveev, V.; Fain, X.; Asaf, D.; Luria, M. Bromine-induced oxidation of mercury in the mid-latitude atmosphere. *Nat. Geosci.* **2011**, *4*, 22–26.
- (6) Lyman, S. N.; Jaffe, D. A. Formation and fate of oxidized mercury in the upper troposphere and lower stratosphere. *Nat. Geosci.* **2012**, *5*, 114–117.
- (7) Ariya, P. A.; Amyot, M.; Dastoor, A.; Deeds, D.; Feinberg, A.; Kos, G.; Poulain, A.; Ryjkov, A.; Semeniuk, K.; Subir, M.; Toyota, K. Mercury Physicochemical and Biogeochemical Transformation in the Atmosphere and at Atmospheric Interfaces: A Review and Future Directions. *Chem. Rev.* **2015**, *115*, 3760–3802.
- (8) Shah, V.; Jacob, D. J.; Thackray, C. P.; Wang, X.; Sunderland, E. M.; Dibble, T. S.; Saiz-Lopez, A.; Cernušák, I.; Kellö, V.; Castro, P. J.; Wu, R.; Wang, C. Improved Mechanistic Model of the Atmospheric Redox Chemistry of Mercury. *Environ. Sci. Technol.* **2021**, *55*, 14445–14456.
- (9) Saiz-Lopez, A.; Travníkov, O.; Sonke, J. E.; Thackray, C. P.; Jacob, D. J.; Carmona-García, J.; Francés-Monerris, A.; Roca-Sanjuán, D.; Acuna, A. U.; Dávalos, J. Z.; Cuevas, C. A.; Jiskra, M.; Wang, F.; Bieser, J.; Plane, J. M. C.; Francisco, J. S. Photochemistry of oxidized Hg(I) and Hg(II) species suggests missing mercury oxidation in the troposphere. *Proc. Natl. Acad. Sci. U.S.A.* **2020**, *117*, 30949–30956.
- (10) Blum, J. D.; Sherman, L. S.; Johnson, M. W. Mercury isotopes in earth and environmental sciences. *Annu. Rev. Earth Planet. Sci.* **2014**, *42*, 249–269.
- (11) Bergquist, B. A.; Blum, J. D. Mass-dependent and -independent fractionation of Hg isotopes by photoreduction in aquatic systems. *Science* **2007**, *318*, 417–420.
- (12) Sun, G.; Sommar, J.; Feng, X.; Lin, C.-J.; Ge, M.; Wang, W.; Yin, R.; Fu, X.; Shang, L. Mass-dependent and -independent fractionation of mercury isotope during gas-phase oxidation of elemental mercury vapor by atomic Cl and Br. *Environ. Sci. Technol.* **2016**, *50*, 9232–9241.
- (13) Zheng, W.; Hintelmann, H. Mercury isotope fractionation during photoreduction in natural water is controlled by its Hg/DOC ratio. *Geochim. Cosmochim. Acta* **2009**, *73*, 6704–6715.
- (14) Motta, L. C.; Blum, J. D.; Johnson, M. W.; Umhau, B. P.; Popp, B. N.; Washburn, S. J.; Drazen, J. C.; Benitez-Nelson, C. R.; Hannides, C. C. S.; Close, H. G.; Lamborg, C. H. Mercury Cycling in the North Pacific Subtropical Gyre as Revealed by Mercury Stable Isotope Ratios. *Global Biogeochem. Cycles* **2019**, *33*, 777–794.
- (15) Sherman, L. S.; Blum, J. D.; Johnson, K. P.; Keeler, G. J.; Barres, J. A.; Douglas, T. A. Mass-independent fractionation of mercury isotopes in Arctic snow driven by sunlight. *Nat. Geosci.* **2010**, *3*, 173–177.
- (16) Wiederhold, J. G.; Cramer, C. J.; Daniel, K.; Infante, I.; Bourdon, B.; Kretzschmar, R. Equilibrium Mercury Isotope Fractionation between Dissolved Hg(II) Species and Thiol-Bound Hg. *Environ. Sci. Technol.* **2010**, *44*, 4191–4197.

- (17) Zheng, W.; Hintelmann, H. Nuclear Field Shift Effect in Isotope Fractionation of Mercury during Abiotic Reduction in the Absence of Light. *J. Phys. Chem. A* **2010**, *114*, 4238–4245.
- (18) Zheng, W.; Demers, J. D.; Lu, X.; Bergquist, B. A.; Anbar, A. D.; Blum, J. D.; Gu, B. Mercury Stable Isotope Fractionation during Abiotic Dark Oxidation in the Presence of Thiols and Natural Organic Matter. *Environ. Sci. Technol.* **2019**, *53*, 1853–1862.
- (19) Gratz, L. E.; Keeler, G. J.; Blum, J. D.; Sherman, L. S. Isotopic composition and fractionation of mercury in Great Lakes precipitation and ambient air. *Environ. Sci. Technol.* **2010**, *44*, 7764–7770.
- (20) Chen, J.; Hintelmann, H.; Feng, X.; Dimock, B. Unusual fractionation of both odd and even mercury isotopes in precipitation from Peterborough, ON, Canada. *Geochim. Cosmochim. Acta* **2012**, *90*, 33–46.
- (21) Demers, J. D.; Blum, J. D.; Zak, D. R. Mercury isotopes in a forested ecosystem: Implications for air-surface exchange dynamics and the global mercury cycle. *Global Biogeochem. Cycles* **2013**, *27*, 222–238.
- (22) Fu, X.; Jiskra, M.; Yang, X.; Maruszczak, N.; Enrico, M.; Chmeleff, J.; Heimbürger-Boavida, L.-E.; Gheusi, F.; Sonke, J. E. Mass-Independent Fractionation of Even and Odd Mercury Isotopes during Atmospheric Mercury Redox Reactions. *Environ. Sci. Technol.* **2021**, *55*, 10164–10174.
- (23) Huang, Q.; Chen, J.; Huang, W.; Fu, P.; Guinot, B.; Feng, X.; Shang, L.; Wang, Z.; Wang, Z.; Yuan, S.; Cai, H.; Wei, L.; Yu, B. Isotopic composition for source identification of mercury in atmospheric fine particles. *Atmos. Chem. Phys.* **2016**, *16*, 11773–11786.
- (24) Xu, H. M.; Sun, R. Y.; Cao, J. J.; Huang, R.-J.; Guinot, B.; Shen, Z. X.; Jiskra, M.; Li, C. X.; Du, B. Y.; He, C.; Liu, S. X.; Zhang, T.; Sonke, J. E. Mercury stable isotope compositions of Chinese urban fine particulates in winter haze days: Implications for Hg sources and transformations. *Chem. Geol.* **2019**, *504*, 267–275.
- (25) Das, R.; Wang, X. F.; Khezri, B.; Webster, R. D.; Sikdar, P. K.; Datta, S. Mercury isotopes of atmospheric particle bound mercury for source apportionment study in urban Kolkata, India. *Elementa* **2016**, *4*, 000098.
- (26) Guo, J.; Sharma, C. M.; Tripathee, L.; Kang, S.; Fu, X.; Huang, J.; Shrestha, K. L.; Chen, P. Source identification of atmospheric particle-bound mercury in the Himalayan foothills through non-isotopic and isotope analyses. *Environ. Pollut.* **2021**, *286*, 117317.
- (27) Rolison, J. M.; Landing, W. M.; Luke, W.; Cohen, M.; Salters, V. J. M. Isotopic composition of species-specific atmospheric Hg in a coastal environment. *Chem. Geol.* **2013**, *336*, 37–49.
- (28) Fu, X.; Zhang, H.; Feng, X.; Tan, Q.; Ming, L.; Liu, C.; Zhang, L. Domestic and Transboundary Sources of Atmospheric Particulate Bound Mercury in Remote Areas of China: Evidence from Mercury Isotopes. *Environ. Sci. Technol.* **2019**, *53*, 1947–1957.
- (29) Yu, B.; Yang, L.; Wang, L.; Liu, H.; Xiao, C.; Liang, Y.; Liu, Q.; Yin, Y.; Hu, L.; Shi, J.; Jiang, G. New evidence for atmospheric mercury transformations in the marine boundary layer from stable mercury isotopes. *Atmos. Chem. Phys.* **2020**, *20*, 9713–9723.
- (30) Qiu, Y.; Gai, P.; Yue, F.; Zhang, Y.; He, P.; Kang, H.; Yu, X.; Lam, P. K. S.; Chen, J.; Xie, Z. Stable Mercury Isotopes Revealing Photochemical Processes in the Marine Boundary Layer. *J. Geophys. Res.: Atmos.* **2021**, *126*, No. e2021JD034630.
- (31) Li, C.; Chen, J.; Angot, H.; Zheng, W.; Shi, G.; Ding, M.; Du, Z.; Zhang, Q.; Ma, X.; Kang, S.; Xiao, C.; Ren, J.; Qin, D. Seasonal Variation of Mercury and Its Isotopes in Atmospheric Particles at the Coastal Zhongshan Station, Eastern Antarctica. *Environ. Sci. Technol.* **2020**, *54*, 11344–11355.
- (32) Zheng, W.; Chandan, P.; Steffen, A.; Stupple, G.; De Vera, J.; Mitchell, C. P. J.; Wania, F.; Bergquist, B. A. Mercury stable isotopes reveal the sources and transformations of atmospheric Hg in the high Arctic. *Appl. Geochem.* **2021**, *131*, 105002.
- (33) Huang, Q.; Chen, J.; Huang, W.; Reinfelder, J. R.; Fu, P.; Yuan, S.; Wang, Z.; Yuan, W.; Cai, H.; Ren, H.; Sun, Y.; He, L. Diel variation in mercury stable isotope ratios records photoreduction of PM_{2.5}-bound mercury. *Atmos. Chem. Phys.* **2019**, *19*, 315–325.
- (34) Amos, H. M.; Jacob, D. J.; Holmes, C. D.; Fisher, J. A.; Wang, Q.; Yantosca, R. M.; Corbitt, E. S.; Galarneau, E.; Rutter, A. P.; Gustin, M. S.; Steffen, A.; Schauer, J. J.; Graydon, J. A.; Louis, V. L. S.; Talbot, R. W.; Edgerton, E. S.; Zhang, Y.; Sunderland, E. M. Gas-particle partitioning of atmospheric Hg(II) and its effect on global mercury deposition. *Atmos. Chem. Phys.* **2012**, *12*, 591–603.
- (35) Fu, X. W.; Zhang, H.; Yu, B.; Wang, X.; Lin, C.-J.; Feng, X. B. Observations of atmospheric mercury in China: a critical review. *Atmos. Chem. Phys.* **2015**, *15*, 9455–9476.
- (36) Wang, X.; Lin, C.-J.; Feng, X.; Yuan, W.; Fu, X.; Zhang, H.; Wu, Q.; Wang, S. Assessment of Regional Mercury Deposition and Emission Outflow in Mainland China. *J. Geophys. Res.: Atmos.* **2018**, *123*, 9868–9890.
- (37) Fu, X.; Liu, C.; Zhang, H.; Xu, Y.; Zhang, H.; Li, J.; Lyu, X.; Zhang, G.; Guo, H.; Wang, X.; Zhang, L.; Feng, X. Isotopic compositions of atmospheric total gaseous mercury in 10 Chinese cities and implications for land surface emissions. *Atmos. Chem. Phys.* **2021**, *21*, 6721–6734.
- (38) Fu, X.; Heimbürger, L.-E.; Sonke, J. E. Collection of atmospheric gaseous mercury for stable isotope analysis using iodine- and chlorine-impregnated activated carbon traps. *J. Anal. At. Spectrom.* **2014**, *29*, 841–852.
- (39) Blum, J. D.; Bergquist, B. A. Reporting of variations in the natural isotopic composition of mercury. *Anal. Bioanal. Chem.* **2007**, *388*, 353–359.
- (40) Blum, J. D.; Johnson, M. W. Recent Developments in Mercury Stable Isotope Analysis. *Rev. Mineral. Geochem.* **2017**, *82*, 733–757.
- (41) Mao, H.; Cheng, I.; Zhang, L. Current understanding of the driving mechanisms for spatiotemporal variations of atmospheric speciated mercury: a review. *Atmos. Chem. Phys.* **2016**, *16*, 12897–12924.
- (42) Åkerblom, S.; Meili, M.; Bishop, K. Organic Matter in Rain: An Overlooked Influence on Mercury Deposition. *Environ. Sci. Technol. Lett.* **2015**, *2*, 128–132.
- (43) Benoit, J. M.; Mason, R. P.; Gilmour, C. C.; Aiken, G. R. Constants for mercury binding by dissolved organic matter isolates from the Florida Everglades. *Geochim. Cosmochim. Acta* **2001**, *65*, 4445–4451.
- (44) Rutter, A. P.; Schauer, J. J. The impact of aerosol composition on the particle to gas partitioning of reactive mercury. *Environ. Sci. Technol.* **2007**, *41*, 3934–3939.
- (45) Xu, H.; Sonke, J. E.; Guinot, B.; Fu, X.; Sun, R.; Lanzanova, A.; Candaudap, F.; Shen, Z.; Cao, J. Seasonal and Annual Variations in Atmospheric Hg and Pb Isotopes in Xi'an, China. *Environ. Sci. Technol.* **2017**, *51*, 3759–3766.
- (46) Yu, B.; Fu, X.; Yin, R.; Zhang, H.; Wang, X.; Lin, C.-J.; Wu, C.; Zhang, Y.; He, N.; Fu, P.; Wang, Z.; Shang, L.; Sommar, J.; Sonke, J. E.; Maurice, L.; Guinot, B.; Feng, X. Isotopic Composition of Atmospheric Mercury in China: New Evidence for Sources and Transformation Processes in Air and in Vegetation. *Environ. Sci. Technol.* **2016**, *50*, 9262–9269.
- (47) Tang, S.; Feng, C.; Feng, X.; Zhu, J.; Sun, R.; Fan, H.; Wang, L.; Li, R.; Mao, T.; Zhou, T. Stable isotope composition of mercury forms in flue gases from a typical coal-fired power plant, Inner Mongolia, northern China. *J. Hazard. Mater.* **2017**, *328*, 90–97.
- (48) Li, X.; Li, Z.; Chen, J.; Zhang, L.; Yin, R.; Sun, G.; Meng, B.; Cui, Z.; Feng, X. Isotope signatures of atmospheric mercury emitted from residential coal combustion. *Atmos. Environ.* **2021**, *246*, 118175.
- (49) Li, X.; Chen, J.; Tang, L.; Wu, T.; Fu, C.; Li, Z.; Sun, G.; Zhao, H.; Zhang, L.; Li, Q.; Feng, X. Mercury isotope signatures of a pre-calciner cement plant in Southwest China. *J. Hazard. Mater.* **2021**, *401*, 123384.
- (50) Zhang, L.; Wang, S.; Wang, L.; Wu, Y.; Duan, L.; Wu, Q.; Wang, F.; Yang, M.; Yang, H.; Hao, J.; Liu, X. Updated Emission Inventories for Speciated Atmospheric Mercury from Anthropogenic Sources in China. *Environ. Sci. Technol.* **2015**, *49*, 3185–3194.
- (51) Fu, X.; Yang, X.; Tan, Q.; Ming, L.; Lin, T.; Lin, C.-J.; Li, X.; Feng, X. Isotopic Composition of Gaseous Elemental Mercury in the

Marine Boundary Layer of East China Sea. *J. Geophys. Res.: Atmos.* **2018**, *123*, 7656–7669.

(52) Fu, X.; Zhang, H.; Liu, C.; Zhang, H.; Lin, C.-J.; Feng, X. Significant Seasonal Variations in Isotopic Composition of Atmospheric Total Gaseous Mercury at Forest Sites in China Caused by Vegetation and Mercury Sources. *Environ. Sci. Technol.* **2019**, *53*, 13748–13756.

(53) Turpin, B. J.; Huntzicker, J. J. Identification of Secondary Organic Aerosol Episodes and Quantitation of Primary and Secondary Organic Aerosol Concentrations during Scaqs. *Atmos. Environ.* **1995**, *29*, 3527–3544.

(54) Tian, H. Z.; Zhu, C. Y.; Gao, J. J.; Cheng, K.; Hao, J. M.; Wang, K.; Hua, S. B.; Wang, Y.; Zhou, J. R. Quantitative assessment of atmospheric emissions of toxic heavy metals from anthropogenic sources in China: historical trend, spatial distribution, uncertainties, and control policies. *Atmos. Chem. Phys.* **2015**, *15*, 10127–10147.

(55) Zheng, W.; Hintelmann, H. Isotope fractionation of mercury during its photochemical reduction by low-molecular-weight organic compounds. *J. Phys. Chem. A* **2010**, *114*, 4246–4253.

(56) Huang, Q.; He, X.; Huang, W.; Reinfelder, J. R. Mass-Independent Fractionation of Mercury Isotopes during Photo-reduction of Soot Particle Bound Hg(II). *Environ. Sci. Technol.* **2021**, *55*, 13783–13791.

(57) Seigneur, C.; Wrobel, J.; Constantinou, E. A Chemical Kinetic Mechanism for Atmospheric Inorganic Mercury. *Environ. Sci. Technol.* **1994**, *28*, 1589–1597.

(58) Seigneur, C.; Abeck, H.; Chia, G.; Reinhard, M.; Bloom, N. S.; Prestbo, E.; Saxena, P. Mercury adsorption to elemental carbon (soot) particles and atmospheric particulate matter. *Atmos. Environ.* **1998**, *32*, 2649–2657.

(59) Rutter, A. P.; Shakya, K. M.; Lehr, R.; Schauer, J. J.; Griffin, R. J. Oxidation of gaseous elemental mercury in the presence of secondary organic aerosols. *Atmos. Environ.* **2012**, *59*, 86–92.

(60) Sun, R.; Streets, D. G.; Horowitz, H. M.; Amos, H. M.; Liu, G. J.; Perrot, V.; Toutain, J. P.; Hintelmann, H.; Sunderland, E. M.; Sonke, J. E. Historical (1850–2010) mercury stable isotope inventory from anthropogenic sources to the atmosphere. *Elementa* **2016**, *4*, 000091.

(61) Motta, L. C.; Kritee, K.; Blum, J. D.; Tsz-Ki Tsui, M.; Reinfelder, J. R. Mercury Isotope Fractionation during the Photochemical Reduction of Hg(II) Coordinated with Organic Ligands. *J. Phys. Chem. A* **2020**, *124*, 2842–2853.

(62) Zhang, H.; Tan, Q. Y.; Zhang, L. M.; Fu, X. W.; Feng, X. B. A Laboratory Study on the Isotopic Composition of Hg(0) Emitted From Hg-Enriched Soils in Wanshan Hg Mining Area. *J. Geophys. Res.: Atmos.* **2020**, *125*, No. e2020JD032572.

(63) Pio, C. A.; Legrand, M.; Oliveira, T.; Afonso, J.; Santos, C.; Caseiro, A.; Fialho, P.; Barata, F.; Puxbaum, H.; Sanchez-Ochoa, A.; Kasper-Giebl, A.; Gelencsér, A.; Preunkert, S.; Schock, M. Climatology of aerosol composition (organic versus inorganic) at nonurban sites on a west-east transect across Europe. *J. Geophys. Res.: Atmos.* **2007**, *112*, D23S02.

(64) Tong, Y.; Eichhorst, T.; Olson, M. R.; McGinnis, J. E.; Turner, I.; Rutter, A. P.; Shafer, M. M.; Wang, X.; Schauer, J. J. Atmospheric photolytic reduction of Hg(II) in dry aerosols. *Environmental Science: Processes & Impacts* **2013**, *15*, 1883–1888.

(65) Lin, C.-j.; Pehkonen, S. O. Aqueous free radical chemistry of mercury in the presence of iron oxides and ambient aerosol. *Atmos. Environ.* **1997**, *31*, 4125–4137.

(66) Li, W.; Shao, L.; Zhang, D.; Ro, C.-U.; Hu, M.; Bi, X.; Geng, H.; Matsuki, A.; Niu, H.; Chen, J. A review of single aerosol particle studies in the atmosphere of East Asia: morphology, mixing state, source, and heterogeneous reactions. *J. Cleaner Prod.* **2016**, *112*, 1330–1349.

(67) Mason, R. P.; Lawson, N. M.; Sheu, G.-R. Mercury in the Atlantic Ocean: factors controlling air-sea exchange of mercury and its distribution in the upper waters. *Deep Sea Res., Part II* **2001**, *48*, 2829–2853.

(68) Feng, X.; Lu, J. Y.; Gregoire, D. C.; Hao, Y.; Banic, C. M.; Schroeder, W. H. Analysis of inorganic mercury species associated with airborne particulate matter/aerosols: method development. *Anal. Bioanal. Chem.* **2004**, *380*, 683–689.

(69) Wang, Y.; Liu, G.; Li, Y.; Liu, Y.; Guo, Y.; Shi, J.; Hu, L.; Cai, Y.; Yin, Y.; Jiang, G. Occurrence of Mercurous [Hg(I)] Species in Environmental Solid Matrices as Probed by Mild 2-Mercaptoethanol Extraction and HPLC-ICP-MS Analysis. *Environ. Sci. Technol. Lett.* **2020**, *7*, 482–488.

(70) Jiang, T.; Skyllberg, U.; Wei, S.; Wang, D.; Lu, S.; Jiang, Z.; Flanagan, D. C. Modeling of the structure-specific kinetics of abiotic, dark reduction of Hg(II) complexed by O/N and S functional groups in humic acids while accounting for time-dependent structural rearrangement. *Geochim. Cosmochim. Acta* **2015**, *154*, 151–167.

(71) Stathopoulos, D. Fractionation of mercury isotopes in an aqueous environment: Chemical Oxidation. Master Thesis, Trent University, Peterborough, Ontario, Canada, 2014.

(72) Fu, B.; Sun, R.; Yao, H.; Hower, J. C.; Yuan, J.; Luo, G.; Hu, H.; Mardon, S. M.; Tang, Q. Mercury stable isotope fractionation during gaseous elemental mercury adsorption onto coal fly ash particles: Experimental and field observations. *J. Hazard. Mater.* **2021**, *405*, 124280.

(73) Kurien, U.; Hu, Z.; Lee, H.; Dastoor, A. P.; Ariya, P. A. Radiation enhanced uptake of Hg-(g)(o) on iron (oxyhydr) oxide nanoparticles. *RSC Adv.* **2017**, *7*, 45010–45021.

(74) Kwon, S. Y.; Blum, J. D.; Yin, R.; Tsui, M. T.-K.; Yang, Y. H.; Choi, J. W. Mercury stable isotopes for monitoring the effectiveness of the Minamata Convention on Mercury. *Earth-Sci. Rev.* **2020**, *203*, 103111.

(75) Enrico, M.; Roux, G. L.; Maruszczak, N.; Heimbürger, L.-E.; Claustres, A.; Fu, X.; Sun, R.; Sonke, J. E. Atmospheric Mercury Transfer to Peat Bogs Dominated by Gaseous Elemental Mercury Dry Deposition. *Environ. Sci. Technol.* **2016**, *50*, 2405–2412.

(76) Jiskra, M.; Heimbürger-Boavida, L.-E.; Desgranges, M.-M.; Petrova, M. V.; Dufour, A.; Ferreira-Araujo, B.; Masbou, J.; Chmieleff, J.; Thyssen, M.; Point, D.; Sonke, J. E. Mercury stable isotopes constrain atmospheric sources to the ocean. *Nature* **2021**, *597*, 678–682.

(77) Sun, R.; Jiskra, M.; Amos, H. M.; Zhang, Y.; Sunderland, E. M.; Sonke, J. E. Modelling the mercury stable isotope distribution of Earth surface reservoirs: Implications for global Hg cycling. *Geochim. Cosmochim. Acta* **2019**, *246*, 156–173.

(78) Selin, N. E.; Jacob, D. J. Seasonal and spatial patterns of mercury wet deposition in the United States: Constraints on the contribution from North American anthropogenic sources. *Atmos. Environ.* **2008**, *42*, 5193–5204.

(79) Obrist, D.; Agnan, Y.; Jiskra, M.; Olson, C. L.; Colegrove, D. P.; Hueber, J.; Moore, C. W.; Sonke, J. E.; Helmig, D. Tundra uptake of atmospheric elemental mercury drives Arctic mercury pollution. *Nature* **2017**, *547*, 201–204.

(80) Zheng, W.; Obrist, D.; Weis, D.; Bergquist, B. A. Mercury isotope compositions across North American forests. *Global Biogeochem. Cycles* **2016**, *30*, 1475–1492.